539.89/.183.3

ELECTRONIC STRUCTURE AND COMPRESSIBILITY OF METALS AT HIGH PRESSURES

L. V. AL'TSHULER and A. A. BAKANOVA

Usp. Fiz. Nauk 96, 193–215 (October, 1968)

I. INTRODUCTION

THE progress attained in high-pressure physics through the use of shock waves[1,2] has made it possible to determine the compression curves of a large number of elements and chemical compounds, up to pressures of several megabars. Particular interesting results were obtained in the last decade in the study of metals with different electronic structures[3-19]. By now, experimental information is available on approximately 50 metals at very high pressures, i.e., for almost any element with a metallic bond.

The accumulation of so much material makes it advantageous to generalize and compare the data on the relative compressibility of metals and to describe systematically the effects of the variation of their electronic structure upon compression.

The scope of the performed research and a general idea concerning the laws governing the compressibility of metals are illustrated by the atomic-volume curves $\mathcal{V}(Z)$ shown in Fig. 1 ($\mathcal{V}$—volume per gram-atom, Z—atomic number of element) corresponding to normal conditions, shock pressures of 1 Mbar, and pressures of 10 Mbar. The latter curve, pertaining to absolute zero temperature, was obtained, just as in[1], by extrapolating the "cold" compression curves obtained from the experimental data to the region of the quantum-statistical pressures and densities, calculated in accordance with the most accurate variant of the statistical theory of the atom[20].

As shown by the configurations of the curves, the atomic volumes of the metals are periodic functions in a wide range of pressures. This periodicity, which reflects the electronic shell structure of the atoms, takes place in spite of the uniformity of the crystal structures of the metals, corresponding in most cases to the close- and closest-packed arrangements. The largest atomic volumes are possessed by alkali metals with filled p-shells and one valence s-electron. Located at the minima of the atomic-volume curves are the elements of groups III and IV for the short periods and the transition metals of group VIII with strongly interacting d-shells for the long periods. On the decreasing branches of the $\mathcal{V}(Z)$ curves are the alkali-earth and transition metals with successively increasing numbers of binding d-electrons. The noble and other simple metals of the B-groups occupy the rising branches of the $\mathcal{V}(Z)$ curves.

Compression of the metals brings together the atoms and increases their exchange-interaction energy, thus causing a broadening and an overlap of the electron energy levels. In final analysis, at very high pressures the individual electron shell structures of the atoms vanish and are replaced by a statistical distribution of the electrons in the field of the atomic nuclei. In these states of matter, the atomic volumes of the elements are described by monotonic almost-linear functions of the atomic number.

The successive smoothing-out of the $\mathcal{V}(Z)$ curves with increasing pressure offers evidence that metals with large atomic volumes under normal conditions have a stronger compressibility. Superimposed on this regularity, which was noted in[21] and in earlier papers by Bridgman, are very appreciable singularities due to realignments occurring upon compression of the electronic structure of the metals. As shown by cesium and cerium as examples[22], such realignments can occur without a change in the symmetry or type of the crystal lattice, and have at the same time all the features of first-order phase transitions.

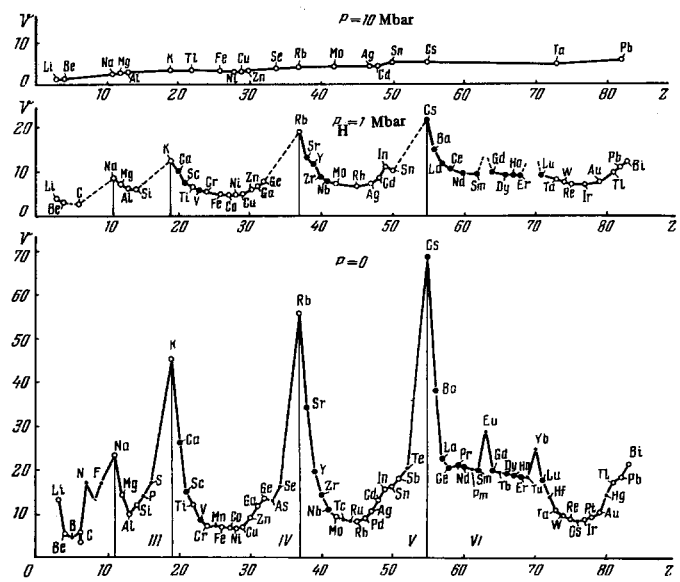

FIG. 1. Dependence of the atomic volumes $\mathcal{V}^0$ of the elements (in cm^3/g-atom) on the atomic number Z under normal conditions for shock compression pressures P_H = 1 Mbar and "cold" compression pressures P_C = 10 Mbar. ●, ○—elements investigated by dynamic methods; ●—metals whose compression curves have singularities connected with electron realignment.

The most probable, in the experimentally attainable range of pressures, are changes of the electronic structure of long-period metals having an inversion with filling of the energy levels. When the atoms come closer together under the influence of the pressure, the outer s-electrons, which are located on the periphery of the electron cloud[23,24], can move towards the inner unfilled d-levels. For alkali metals, these phenomena were considered theoretically in[25], and in particular detail, with potassium as an example, in[26] (Fig. 2a). Under normal conditions, the Fermi surface of potassium passes through the middle of the partly filled 4s-band and below the empty 3d-band, which consists of several energy subbands. Upon compression, the relative position of the bands changes resulting in final analysis in the sequence characteristic of hydrogen-like atoms.

The transition of the s electrons to the d levels is accompanied by a decrease of the limiting density of the electrons. The compression curve of potassium (Fig. 2b) in the transition region, in analogy with the Van der Waals isotherms, contains an instability interval. The states actually realized are those corresponding to two electronic phases with different volumes, which are in thermodynamic equilibrium. In the first of them the electrons are in the s band, and in the second in the d band. According to[27], a jumpwise repopulation of the electrons always takes place upon intersection of sufficiently narrow bands.

A different picture should be expected in all types of transition metals, where under normal conditions the stable states are those with partial filling of both the s and the d bands. The relative locations of the bands[24,28,29] are shown schematically in Fig. 3. The presented scheme agrees satisfactorily with the experimental data on the average atomic magnetic moments for ferromagnetic metals, on the electronic specific heat and on the paramagnetic susceptibility of paramagnetic metals. In this case, when pressures are applied, the singularities on the compression

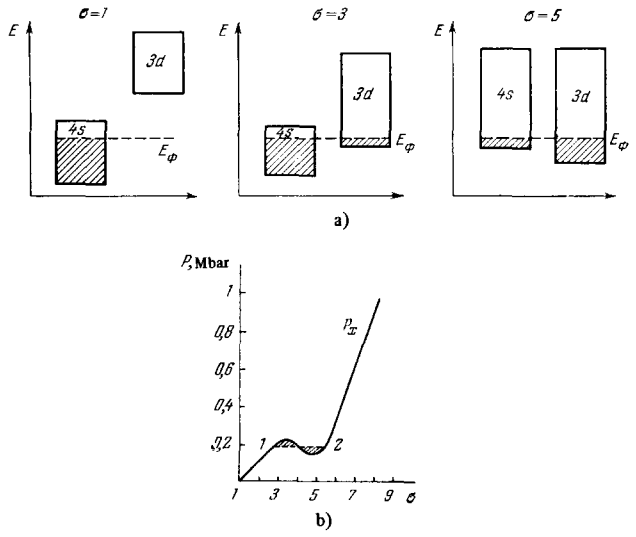

FIG. 2. Electronic transition in K (from [26]). a)Energy spectra of K at normal density and compression by a factor 3 and 5; b) calculated compression curve P(σ) of K for T = 0°K (σ = V_0/V); 1 and 2—stable states at σ = 2.8 and 5.5 corresponding to unfilled d and s bands.

curves[16-19] appear probably at the end of the transition process of the s electrons to the d levels, when the bottom of the broad s-band becomes separated from the Fermi surface.

Effects connected with the displacement of the s electrons are most prevalent and, as shown in Fig. 1, are characteristic of metals located on the decreasing branches of the atomic-volume curve. They do not exhaust, however, all the situations arising upon compression of metals as a result of the intersection of the energy bands and of the change of the topology of the Fermi surface[30].

Many interesting phenomena in the behavior of compressed metals were revealed, in particular, by calculation of their energy spectrum in the Wigner-Seitz spherical-cell approximation, using the procedure of[31].

In the present review we pay principal attention to experimental research. Since the main information on the compressibility of metals at the highest pressures was obtained by dynamic methods, in Section II we present a brief exposition of the shock-wave method and of the main features of the shock-compression processes. The concise character of the exposition of these questions is due to the presence of a survey[1] and other publications[2,33] devoted to shock waves and their use in high-pressure physics. Subsequent sections of the review will be devoted to the results of investigations of simple, transition, alkali-earth, alkali, and rare-earth metals.

II. THE SHOCK-WAVE METHOD

In order to carry out dynamic investigations, shock waves are used, produced by decelerating detonation waves by partitions[3-5], by encounter of bodies accelerated by explosion products with immobile target-samples[4-19,34], and by diverging waves produced by strong underground explosions[35,36]. A shock wave is a strong disturbance that propagates in a medium at supersonic velocity. The velocity D of the wave front and the velocity u of the translational motion of the particles of the medium behind its front determine[1-4] the sought thermodynamic parameters of the substance compressed and heated by the shock wave, namely its specific volume V, pressure P, and internal energy E. If in the initial state (denoted by the index 0) the substance is at rest and is not compressed, then behind the wave front

$$V=V_0(D-u)D^{-1},\quad P=v_0^{-1}Du,\quad E=E_0+\frac{u^2}{2}=E_0+\frac{1}{2}P(V_0-V). \quad (1)$$

The relations (1) express the conditions for the conservation of mass, momentum, and energy. The states

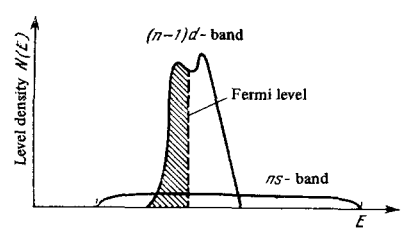

FIG. 3. Schematic diagram of filling of the bands of transition metals under normal conditions. n—principal quantum number.

occurring upon motion of waves of different amplitude are described by the shock adiabat of the material—the Hugoniot adiabat. On the schematic P-V diagram of Fig. 4a, the shock adiabat (upper curve) is shown together with the zero isotherm characterizing the "cold" resistance of the medium at absolute zero temperature. With increasing shock-wave amplitude, the fraction of the thermal components in the pressure and energy increases progressively and in final analysis becomes dominating. To the contrary, at not very large compressions, the role of the heat is relatively small. In this case the shape of the adiabats is determined primarily by the course of the "cold" compression curves, reflecting all the singularities inherent in these curves.

Shock adiabats describing processes of non-isentropic heating, are always steeper than the isentropes (see Fig. 4a). There exists a simple relation[10,19] which connects the slopes of the Hugoniot adiabats and the isentropes at the points of their intersection. In terms of the variables P, $\sigma = V_0/V$

$$(h-\sigma)\left(\frac{\partial P}{\partial \ln \sigma}\right)_H = (h-1)\left(\frac{\partial P}{\partial \ln \sigma}\right)_S - P(\sigma). \qquad (2)$$

In (2), $(\partial P/\partial \ln \sigma)_S$ is the isentropic modulus of volume compression; $h = 1 + 2/\gamma$; γ—dimensionless coefficient determining the ratio of the thermal pressure to the volume concentration of the thermal energy and characterizing the thermal elasticity of the substance.

If the Hugoniot adiabat has points at which the values of $(dP/d\ln\sigma)_H$ experience discontinuities (see Fig. 4b) then, according to (2), the corresponding differences of the isentropic moduli are

$$\Delta\left(\frac{\partial P}{\partial \ln \sigma}\right)_S = \frac{h-\sigma}{h-1}\Delta\left(\frac{\partial P}{\partial \ln \sigma}\right)_H. \qquad (2a)$$

Since the fractional coefficient in the right side of (2a) is smaller than unity, the breaks of the adiabats are always larger than the breaks of the isentropes.

In the presence of projections on the zero isotherms((see Fig. 4c), which are characteristic of first-order phase transitions, we encounter the opposite picture of partial smoothing of these effects when recorded by dynamic methods. The smoothing is the result of the non-isothermal nature of the transitions under shock compression[1], owing to the temperature smearing of the band boundaries[27] (for electronic transitions), and, finally, as the result of the inertial character of the phase transitions.

In the latter case, dynamic experiments at supercritical pressures record sequences of nonequilibrium states (see the dashed line in Fig. 4c), corresponding to mixtures of phases of high and low pressures.

As shown by Fig. 4a, certain characteristic degrees of compression $\sigma_{tr} = V_0/V_{tr}$ on the vertical sections of the adiabats, the increase of the shock pressure is completely balanced by the equal increase of the thermal pressure

$$\Delta P_T = \frac{\gamma}{V_{tr}}\Delta E_T = \frac{\gamma}{V_{tr}}\Delta P\frac{V_0 - V_{tr}}{2}$$

(see equation (1)).

It can be easily seen, that the equality of the quantities ΔP_T and ΔP is satisfied only when $\sigma_{tr} = 1 + (2/\gamma) = h$, which follows also from (2). The presence of limiting degrees of compression[2] is a characteristic feature of shock adiabats and has no analogues in the isentropic and isothermal processes, where the increase of the pressure always leads to a decrease of the volume. For bound weakly-degenerate electrons in a Coulomb field of nuclei, the limiting compression is ~5. Further increase of the temperature imparts to the metal the properties of a monatomic ideal gas, for which $\sigma_{tr} = 4$. At still higher temperatures of shock compression, when the bulk of the energy goes over into radiation, $\sigma_{tr} = 7$. Metals reach their first limiting state with $\sigma_{tr} \approx 5.0$ at shock-wave amplitudes equal to several hundreds of megabars of thermal pressure.

In the present review we are interested primarily in much lower pressures of the lower parts of the adiabats in that region where their course does not differ greatly from the course of the zero isotherms.

The possibilities of experimentally reaching the region of high pressures with the aid of dynamic methods is illustrated by the $P - \sigma$ diagram of Fig. 5, which shows Hugoniot adiabats of Fe and Pb. Up to 10 Mbar, the determined compressibilities of Fe and Pb or of other metals have an absolute character, since they are based on an independent determination of the wave and mass velocities of shock waves of different amplitudes[1,4].

To obtain experimental information in the indicated range of pressures, it is necessary to determine first the shock adiabats of a small number of standard metals (Fe, Al, Cu) by recording, with the scheme of Fig. 6, the wave velocities in the targets and the velocities of the bodies striking the targets. To per-

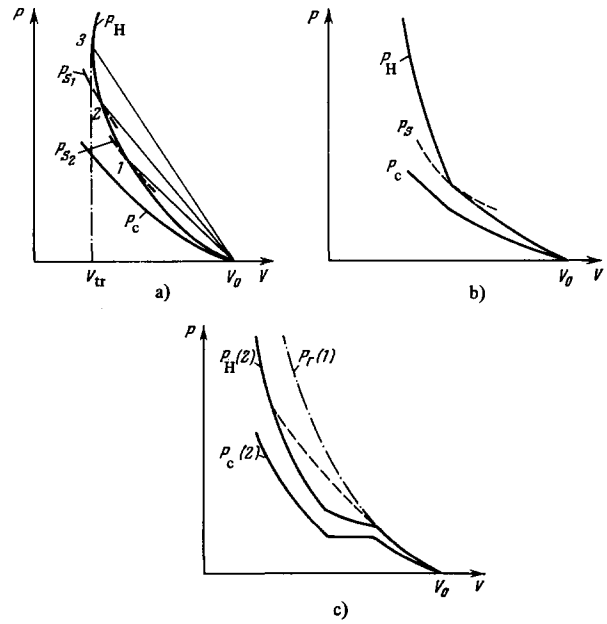

FIG. 4. Schematic P-V diagrams of shock compression. P_H—shock adiabats; P_C—zero isotherms determining the resistance of the medium to "cold" compression at T = 0°K; P_{S_1} and P_{S_2}—isentropes; 1–3—states of shock compression for waves of different amplitude: a)smooth compression curves; b) compression curves with kinks; c) zero isotherms and Hugoniot adiabats in the presence of a phase transition; —·— metastable branch of Hugoniot adiabats of first phase, —— nonequilibrium adiabat of a mixture of low and high pressure phases.

form these measurements, Soviet investigators used in the late 40's explosion systems developed by them, which impart to the strikers velocities reaching 8–14 km/sec[4,7,9,11,13].

In 1962[12], velocities on the order of 8 km/sec were obtained by British scientists using hemispherical cumulative charges, which accelerate thin-wall steel shells embedded in them and strike in synchronism against segments of the investigated materials.

Another method, with the aid of small tungsten missiles shot from a long-barrel "light-gas" gun, yielded similar results, 8.0 km/sec (6 Mbar) in 1966 in the USA[34] in a study of tungsten and gold.

The compression parameters of most metals were determined by a differential method[3,5] by comparing the velocities of the shock waves passing successively through standards and the investigated metals. A differential method was also used to determine the comparative compressibility of Fe and Pb[36] at the highest pressures, 30 Mbar, which go far beyond the region of absolute measurements.

In these still unique experiments, they determined the velocity of a strong shock wave of an underground explosion, passing through layers of Fe and Pb. In the interpretation of the obtained data, the Pb was considered as the standard substance, whose shock adiabat at 30–40 Mbar was obtained by extrapolation and was assumed to be known. As seen from the relative positions of the adiabats, the compressibilities of Fe and Pb are quite different. The same pressure, 30 Mbar, increases the density of Pb by 3.3 times and that of Fe by only 2.5 times.

The curves of "cold" compression of Fe and Pb are arranged in a manner similar to the adiabats. These relations were obtained by resolving the total shock pressure into a thermal and "cold" component by the methods described in[1-3,7-11].

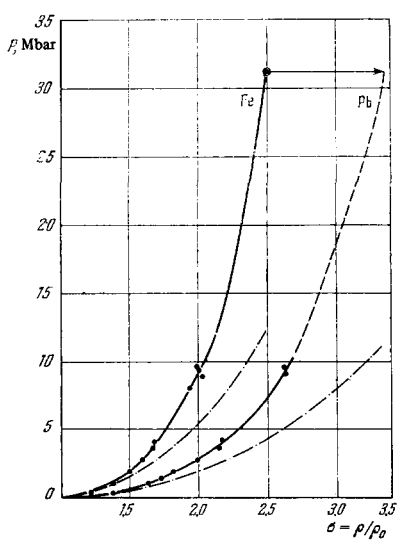

FIG. 5. Shock adiabats (P_H) and "cold" compression curves (P_C) of Pb and Fe. – P_H; –·– P_C; – – extrapolated section of shock adiabat of Pb; ●–data of absolute measurements [3–9,12,13]; ⊙–results of determination of the relative compressibility of Pb and Fe [36].

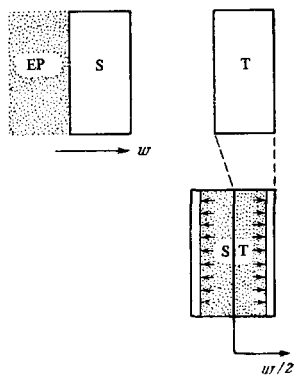

FIG. 6. Scheme for absolute determination of the dynamic compressibility of standard metals. EP–explosion products accelerating the striker; S–striker, T–target made of the same material as the striker. The experimentally measured quantity is the velocity of the shock wave in the target and the travel velocity of the striker w = 2u; u–mass velocity of the matter behind the front of the shock wave.

III. COMPARATIVE COMPRESSIBILITY OF SIMPLE METALS

In this section we consider the metals investigated in[3,5,7-9,11-12], which belong to groups B of the periodic table. These include the noble metals (Cu, Ag, Au) and the metals of groups IIB, IIIB, and IVB. Most of them have in the initial state a close or nearly close packed structure. The only exceptions are Ga and Sn.

According to the universally held notions, all the foregoing metals with the exception of Al have filled d-bands and different numbers of valence s-p electrons, equal to the number of the group to which the metal belongs. Unlike the p-shells of the inert gases and ions of the alkali metals, the filled d-shells of the ion cores of the noble metals have a strong exchange interaction[28,29]. As a consequence, the metals of group IB have high coordination numbers, low atomic volumes, and a low compressibility. The increase of the number of s- and p-electrons in metals of groups IIB–IVB weakens the interaction between the d-shells and leads to appearance of more and more friable and compressible structures. A similar sequence in the change of properties is retained also at high pressures, as is evidenced by Figs. 7–9. The abscissas on these figures show the relative densities σ and the ordinates the shock-compression pressures. Figure 7 characterizes the relative compressibility of metals of groups IB, IIB, and IVB up to pressures of 5 Mbar[3,5,7-9,11]. The least compressible are gold, silver, and copper, and the most compressible are lead and tin. Whereas application of shock pressures of 5 Mbar to gold increases its density by 1.65 times, the increase in lead is by 2.29 times. The metals of group IIB, Cd and Zn, occupy an intermediate position.

The authors of[36] traced the comparative compressibility of Pb, Cd, and Cu up to much higher pressures, 14–16 Mbar, using methods described in their paper (Fig. 8). We call attention to the smooth course of the adiabats and to the conservation of their relative positions in a very wide range of pressures. Besides the Hugoniot adiabats, the dash-dot lines show the cold-compression curves for Cu and Cd as obtained in[9,11] by subtracting the thermal components from the shock pressures.

Comparison of the $P_C(\sigma)$ and $P_H(\sigma)$ curves shows that heat assumes an increasing role. At 15 Mbar, the fraction of the thermal pressures amounts to 55% for Pb, 53% for Cd and 45% for Cu. The relative role of the

heat in the total energy of shock compression E_H is even more appreciable, approaching 70–90%.

In the case of elements of group IIIB (Al, Ga, In, and Tl), the initial atomic volume of In differs little from the atomic volume of Sn (see Fig. 1). The same ratio of the volumes holds true for thalium compared with Pb. The shock adiabats of In and Tl (Fig. 9) are respectively similar to the adiabats of Sn and Pb.

Located next to them are also the compressibility curves of Al and Ga. In the case of Al, the shock adiabat is smooth only up to 2 Mbar. At higher pressures, as shown by the data of[12] and of the present authors, the adiabat of Al experiences an inflection. According to[26], at normal density and at degrees of compression $\sigma < 2$, the electrons of Al occupy, besides the filled 3s band, also levels of the $3d_0$ band with large values of the quasimomentum. Further compression leads to a strong increase of the level density near the Fermi surface. The compressibility of the metal then increases, and an inflection appears on the cold-compression curve and leaves its imprint also on the dynamic adiabat of aluminum.

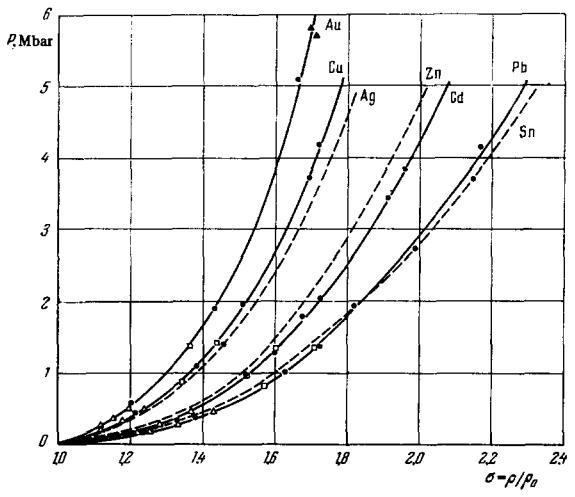

FIG. 7. Dynamic compressibility of simple metals of groups IB, IIB and IVB. Data: ●–Soviet authors [5,7,9,11] □–[8], Δ–[3] ▲–[34](for Au).

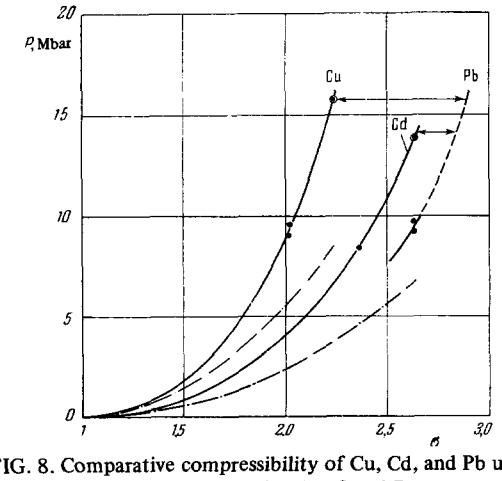

FIG. 8. Comparative compressibility of Cu, Cd, and Pb up to 15 Mbar. The notation is the same as in Figs. 5 and 7

IV. ELECTRON REALIGNMENTS AND COMPRESSIBILITY OF TRANSITION METALS

A more detailed analysis[28] shows that the energy spectra of transition metals consist of a broad s-band and two subbands of the d-band—triple and double, the coupling parts of which may contain three or two electrons each. Under normal conditions, the s and d bands overlap (see Fig. 3).

The fully coupling parts of the d-bands are filled in metals of group VI (Cr, Mo, W), which have the largest

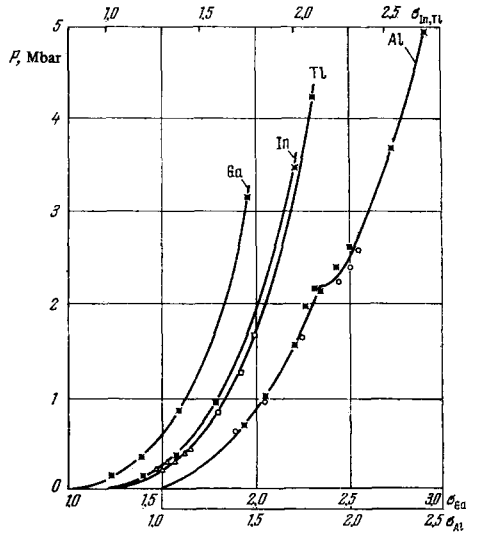

FIG. 9. Shock adiabats of elements of group IIIB. Data: ●–[9,11] ⊙–[12]; remaining notation is the same as in Fig. 7. The shock adiabats are in accordance with Eq. (4): for aluminum $D_I = 5.35 + 1.33u$ at $u < 6$ km/sec; $D_{II} = 5.33 + 1.65u$ at $u > 6.5$ km/sec. For gallium $D = 1.54 + 2.55u$, and for indium $D = 2.62 + 1.468u$.

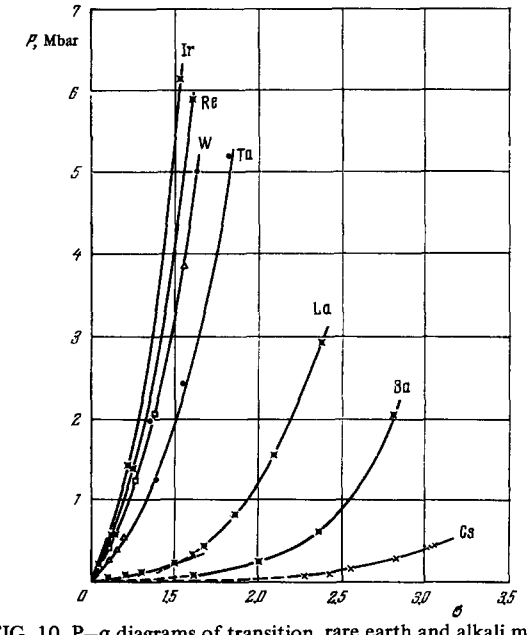

FIG. 10. P–σ diagrams of transition, rare earth and alkali metals of period VI. Data: ●–[16,17,19]; X–[14] (for Cs); ●–[10,13]; the remaining notation is the same as in Fig. 7. $D = 4.03 + 1.414u$ for Re and $D = 3.93 + 1.58u$ for Ir.

adhesion energies. With further filling of the "loosening" parts of the bands, the coupling energies decrease, the coupling becomes less directional, the coordination numbers increase, but the atomic volumes decrease, reaching a minimum in the elements of group VIII.

As shown by experiment[3,4,8-13,19], in each of the periods the compressibility of the transition metals is directly related to their initial atomic volumes, and does not depend directly on the coupling energies. This law is manifest most clearly for metals of periods VI and V (Figs. 10 and 11), which have rather sharply pronounced minima on the $\mathcal{V}(Z)$ curve. Thus, in the case of transition metals of the period VI (Fig. 10) the least compressible is Ir, followed in exact sequence of increasing atomic volume, by Re, W, Ta, and La, which is the representative of the trivalent lanthanides.

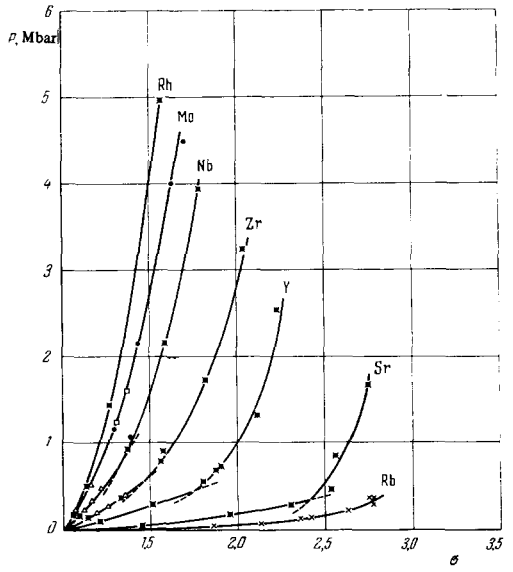

FIG. 11. P–σ diagrams of transition, alkali, and alkali-earth metals of Period V. The notation is the same as in Fig. 10: D = 4.53 + 1.593u for Rh.

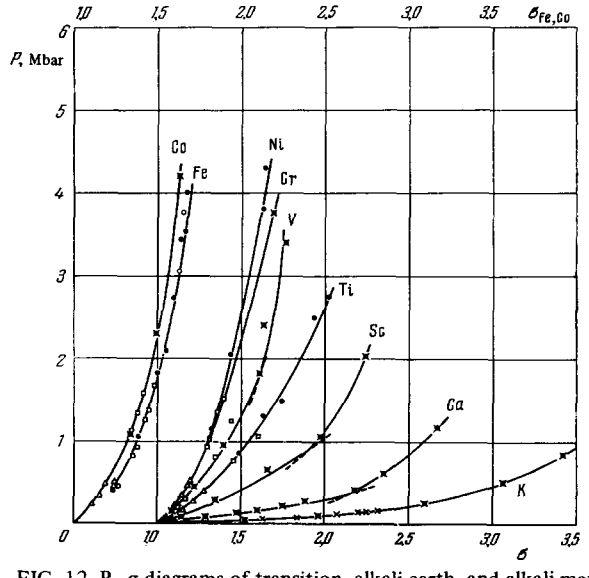

FIG. 12. P–σ diagrams of transition, alkali-earth, and alkali metals of period IV. The notation is the same as in Fig. 10. Data: ✕—for K [15]; ○—Fe [12].

Tungsten has a larger compressibility in spite of the fact that its coupling energy (210 kcal/mole) is practically double the coupling energy of Ir (120 kcal/mole). A similar situation is observed (Fig. 11) also in period V for Rh, with a coupling energy of 110 kcal/mole and atomic volume 8.3 cm^3/mole and Mo with coupling energy 160 kcal/mole and atomic volume 9.34 cm^3/mole, followed by the adiabats of Nb, Zr, and Y, with initial atomic volumes 10.83, 14.02, and 19.88 cm^3/mole.

It is much more difficult to delineate the compressibilities of iron-group metals (Fig. 12) Cr, Fe, Co, and Ni, which have nearly equal initial atomic volumes. The adiabats of these metals are superimposed and cross each other. Following them, in inverse sequence of atomic numbers, are the curves for V, Ti, and Sc, the slopes of which decrease continuously.

The Hugoniot adiabats of the transition metals greatly differ from each other in their configuration. Metals located near the minima of the atomic volumes have adiabats in the form of smooth curves of the parabolic type. An entirely different picture[19] is observed for elements with a small number (1–3) of d-electrons, namely Sc, V, Y, Zr, and Nb. The adiabats of these metals consist of two sections—a lower, gently sloping one, and an upper one which is directed steeply upward.

The kinks on the Hugoniot adiabats, which indicate a discontinuous increase of the elasticity of the metal, are most clearly pronounced if the adiabats are plotted in terms of the kinematic D-u coordinates.

By means of (1), the D-u diagrams determine the parameters of the shock compression, while Eq. (3) determines the slopes of the shock adiabats

$$\left(\frac{\partial P}{\partial \sigma}\right)_H = \frac{(D+D'_u u)(D-u)^2}{(D-D'_u u)V_0} \qquad (3)$$

in P-σ coordinates. When the zero isotherms have a smooth variation, the D-u plots of the metals, unlike the parabolic P-V and P-σ diagrams, are described by a monotonic almost-linear relation. In the monotonic region, they are usually well approximated by relations

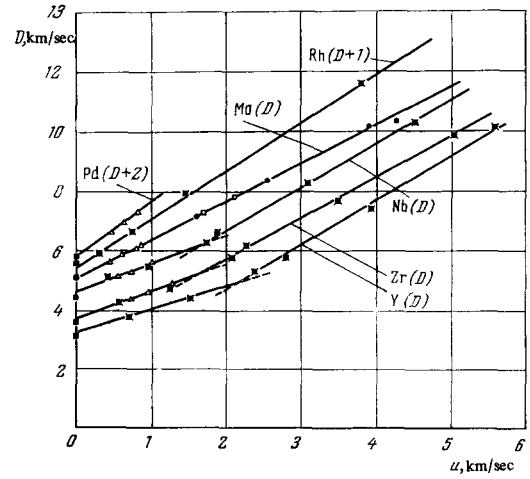

FIG. 13. D-u diagrams of transition metals of period V. Notation is the same as in Fig. 10.

of the type

$$D = C_0 + \lambda u \qquad (4)$$

with a constant value of the derivative $D'_u = \lambda$. Expressions of the type (4) are the most laconic method of describing shock adiabats. The appearance of projections, kinks, or other deviations from linearity on the D-u curves indicate changes in the crystalline or in the electronic structure of the compressible metal.

For elements of the period V, Fig. 13 shows D-u diagrams of six investigated transition metals. For Mo, Rh, and Pd, the D-u plots are described throughout by common linear relations of the type (4). To the contrary, in the case of Y, Zr, and Nb the experimental points lie on two intersecting segments with different inclinations. A similar form is possessed by the D-u plots of Sc, V[19] and La[16]. The slopes of the right-hand sections, corresponding to larger compressions and pressures, are always larger than the slopes of the left-hand sections, and are approximately the same for the different metals. The characteristics of the kink points are determined by the intersection of the left and right sections of the D-u diagrams and subsequent calculation using equations (1) and (3).

The results of these determinations for Sc, V, Y, Zr, Nb, and La are shown in Table I. For each metal, the table lists the pressures and the relative compressions of the critical states and the slopes $(dP/d\sigma)_{H_1}$ and $(dP/d\sigma)_{H_2}$ of the shock adiabats to the left and to the right of the kink points. The table also lists the probable phase states at the critical points and the initial crystalline structures of the elements under consideration. In absolute magnitude, the jumplike changes of the slopes are quite different, differing from each other by more than one order of magnitude. According to estimates[19] based on relation (2a), they exceed by 1.2–1.6 times the discontinuities of the derivatives of the isentropes passing through the kink points. At the lowest pressures, 220 kbar, the transition into the low-compressibility state is observed in La, and at the lowest degrees of compression ($\sigma = 1.35$), in Nb. Both metals are then in the solid state. To the contrary, for the remaining four metals, a jumplike decrease of the compressibility occurs in the region of the liquid phase. The kink of the adiabats is most strongly pronounced for Sc and Y, which have the largest critical value σ_c, and less pronounced in La and Nb. We see that the critical parameters of the metals under consideration are quite different. The only feature they have in common is that all metals having kinks lie on the descending branches of the atomic volumes, and consequently in all these metals the repopulation of the s-electrons on the coupling d-levels is connected with an increase of the coupling forces and with a decrease of the effective dimensions of the atoms. The only metal which does not fit this scheme is titanium, the compression curve of which has a monotonically increasing slope, up to 3 Mbar.

This regularity makes it possible to connect with full justification the presence of the kinks on the compression curves with changes of the electronic structure of the transition metals. From this point of view, the gently sloping initial sections of the adiabats are due not only to the strong compressibility of the external s-electrons, but also to the continuous transition of these electrons to the d-levels. The occurrence of kink points is connected with the completion, under definite degrees of compression, of the process of repopulation of the s electrons and formation of low-compressibility electronic configurations. Electronic realignments of this type also probably occur at various pressures in the transition metals of groups VI–VIII. Inasmuch as the increase of the number of d-electrons has practically no affect on the metal density in this case, these transitions are not recorded experimentally.

V. EFFECT OF HIGH PRESSURES ON ALKALI AND ALKALI-EARTH METALS

The relative arrangement of the shock adiabats[3,12,17,19] of five alkali-earth metals is shown in P-σ diagrams in Fig. 14. The least compressible among them are Be and Mg, which have under normal conditions small atomic volumes. The appreciable coupling energy of these metals and the lower compressibility are connected with the existence of strong covalent bonds, formed by the directed s-p orbitals. In the case of three other alkali-earth metals[17,19], namely Ca, Sr, and Ba, the compressibilities are much larger and are approximately equal. In Figs. 10–12 the adiabats of Ca, Sr, and Ba are located lower than the adiabats of the transition metals of group III, and much higher than the compression curves of the alkali metals.

As is well-known, Be and Mg have a hydrogen-like sequence of electron arrangement. This causes the smoothness of their adiabats. As shown by Figs. 14

Table I

Metal	ρ_0, g/cm³	Lattice type	Parameters of critical states				Probable phase state
			P_k, kbar	σ_k	$\left(\frac{dP}{d\sigma}\right)_{H_1}$, 10^2 kbar	$\left(\frac{dP}{d\sigma}\right)_{H_2}$, 10^2 kbar	
Sc	3.09	HCP	910	1,90	11,0	24,0	L
V	6.08	BCC	1640	1,58	40,0	64,5	L
Nb	8.58	BCC	860	1,35	29,0	39,0	S
Zr	6.51	HCP	530	1,44	14,5	20,0	S
Y	4 49	HCP	460	1,74	7,0	15,0	L
La	6.15	HCP	220	1,51	5,6	8,3	S
Ca	1.62	FCC	390	2,15	4,5	9,0	L
Sr	2.60	FCC	330	2,40	3,5	15,0	L

Symbols for lattice types: HCP–hexagonal close packed, BCC–body centered cubic, FCC–facecentered cubic. Symbols for phase states: S–solid state, L–liquid state.

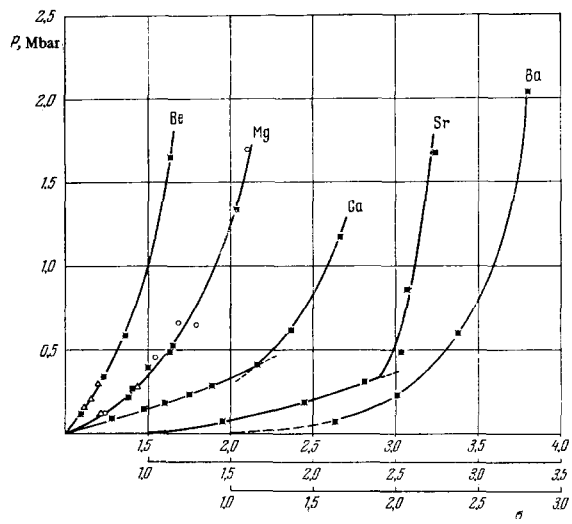

FIG. 14. P–σ diagrams of alkali-earth metals. Data: ●–[17,19]; ○–for Mg [12]; Δ–for Be and Mg [3].

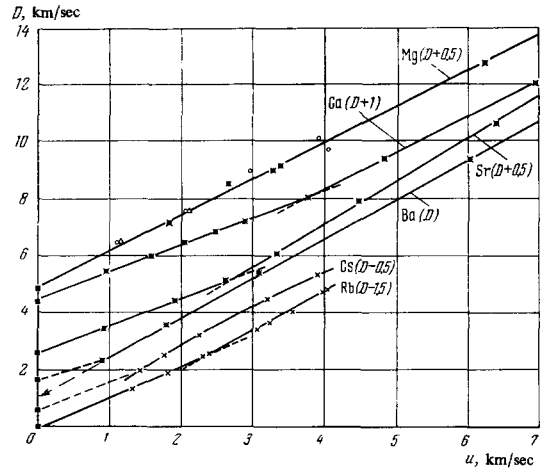

FIG. 15. D-u diagrams of alkali and alkali-earth metals. Notation is the same as in Fig. 14. X–for Rb and Cs [14].

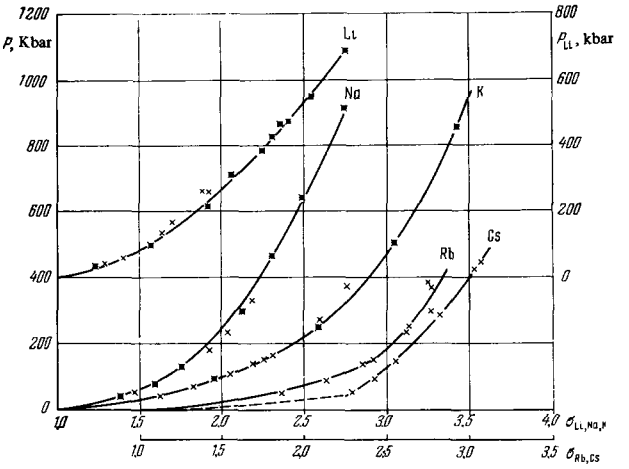

FIG. 16. P–σ diagrams of alkali metals: X–[14], ●–[16].

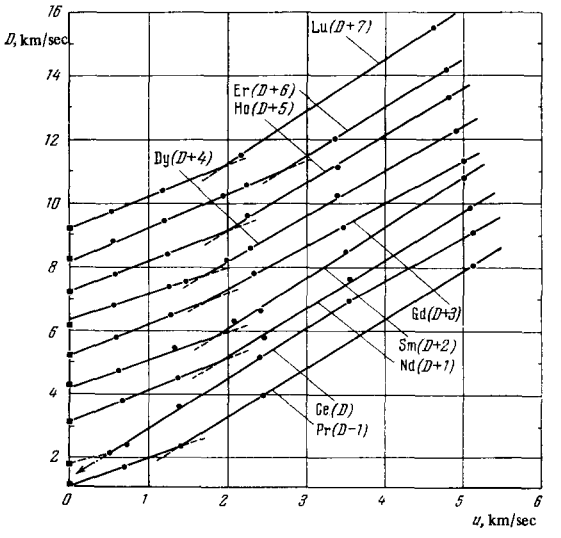

FIG. 17. D-u diagrams for lanthanides: ●–experimental data [16,19].

and 15, perfectly distinct transitions in low-compressibility states are recorded for Ca and Sr at pressures 390 and 330 kbar respectively*. The parameters of the critical states are listed in Table I. According to the classification of Delinger[28], Ca, Sr, and Ba are transition metals, since their metallic properties are the results of partial overlap of their ns and (n – 1)d energy bands (n–number of the period). The compression of the metals leads to a broadening of the energy bands and to a change of their mutual positions–their arrangement approaches the sequency of hydrogen-like atoms. Just as in the case of the transition metals, the formation of low-compressibility phases is connected in these metals with the repopulation of the s-electrons to the d levels.

In the case of Ba, the electronic transition proposed in[37,33] and revealed by the resistance jumps occurs in the solid phase at pressures 140 kbar. The experimental points of the dynamic measurements, as shown by the P-T diagram of Ba[19,22], lies above its melting curve and characterizes a low-compressibility phase. This is evidenced by the slope of the D-u line and its extrapolation to zero values (Fig. 15). The D-u line of Ba crosses the ordinate axis at 550 m/sec below its true speed of sound under normal conditions.

Alkali metals are characterized by a purely metallic type of bond, effected by the s-electrons of the outer shells. These monovalent metals are characterized by small coupling energies and large interatomic distances. On the atomic-volume curve they occupy the extreme uppermost positions. Compared with the metals of all other types, the alkali metals are the most compressible both at low and high pressures. This is evidenced by data of earlier static investigations[38] and by dynamic experiments[1,14,15], represented in Fig. 16, and in the case of K, Rb, and Cs, in addition, on Figs. 10–12. As shown by the adiabats, the compressibility of the alkali metals increases with increasing atomic number, owing to the screening influence of the internal electronic layers. The difference revealed by this attribute is particularly large between Li and

*Under isothermal compression at 20°C, the jumps of the electric resistance are noted in Ca at 380 kbar and in Sr at 50 kbar. [22,33]

Na, on the one hand, and K, Rb, and Cs on the other.

Among the alkali metals, the transitions that lead to a displacement of the s electrons to the d levels are possible in the case of K, Rb, and Cs. In Cs, an isomorphic transformation of the electronic type, accompanied by change of the volume, has been recorded at 45 kbar[38]. At higher dynamic pressures, no further violations of the monotonicity are observed on the Cs adiabat (see Figs. 15 and 16). In Rb, on the basis of the theoretical analysis of the question in[21], the expected pressure of the s-d transition is approximately 200 kbar. At approximately this pressure, the D-u diagram of Rb (Fig. 15) may reveal a weak kink, noted by the authors of[14], and a jump also appears in the electric resistivity[33].

The adiabat of K has a smooth form in a wide range of densities, up to $\sigma = 3.4$[15] (see Fig. 16). In this case we have a certain contradiction to the theory developed in the introduction[26], according to which the formation of a second denser electronic phase of K should begin at $\sigma = 2.8$. It is possible that the observed discrepancy is due to the inaccuracy of the theoretical calculations. It is also possible that the influence of very high temperatures of shock compression of K, which reach several electron volts[15], come into play here. At such high temperatures, there is a strong smearing of the energy bands of the metal, and, as a consequence, the effects of the electronic transitions are suppressed and smoothed out.

VI. ELECTRONIC REALIGNMENTS IN RARE-EARTH METALS

From among the 15 rare-earth metals that occupy the positions between Ba and Hf in the periodic table, the high-pressure shock-compression behavior has been described in[16,18,19] for Pr, Ce, Nb, Sm, Gd, Dy, Ho, Er, and Lu.

The D-u diagrams of these metals are shown in Fig. 17, and the p-σ diagrams (for eight of them) are shown in Figs. 18 and 19. Under normal conditions the rare-earth metals crystalize in different close-packing variants, and, with the exception of Eu and Y, are trivalent metals with very similar chemical properties.

With increasing atomic number, in accordance with the "lanthanum compression" effect, the initial atomic volumes of the rare metals and their compressibility decreases somewhat. As shown by Table II, the application of pressures of 200 kbar to La increases its density by 1.49 times, and in the case of Lu by only 1.31 times.

In all rare earth metals with the exception of Ce, the P-σ and D-u diagrams show discontinuous changes of the compressibility at the parameters indi-

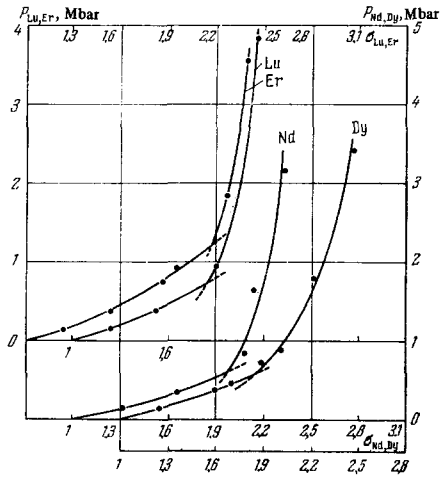

FIG. 18. Shock adiabats of Ho, Ce, Sm and Dy. The notation is the same as in Fig. 17.

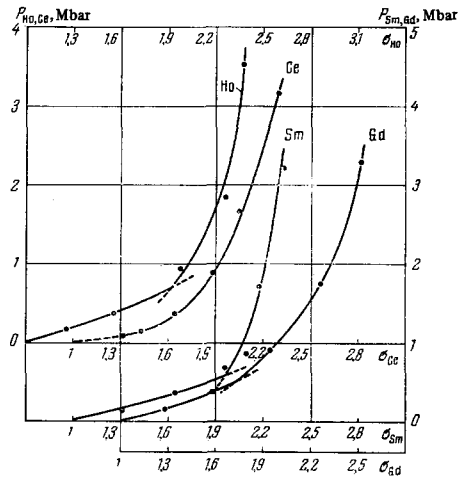

FIG. 19. Shock adiabats of Er, Lu, Nd, and Ge. The notation is the same as in figure 17.

Table II

Z	Element	Lattice type	$\mathcal{V}_0$, $\frac{cm^3}{g\text{-atom}}$	σ at pressure 200 kbar	Parameters of critical states				Probable phase states
					P_{k_1}, kbar	σ_k	$\left(\frac{dP}{d\sigma}\right)_{H_1}$, 10^2 kbar	$\left(\frac{dP}{d\sigma}\right)_{H_2}$, 10^2 kbar	
57	La	HCP	22.54	1.49	220	1.51	5.6	8.3	S
58	Ce-γ	FCC	20.69	1.54	—	—	—	—	—
59	Pr	HCP	20.82	1.51	330	1.76	5.7	12.6	L
60	Nd	HCP	20.59	1.45	610	1.98	9.5	26.0	L
62	Sm	R	19.95	1.43	540	1.95	7.0	24.0	L
64	Gd	HCP	19.94	1.38	545	1.78	10.0	15.0	L
66	Dy	HCP	18.99	1.36	540	1.83	7.8	16.5	L
67	Ho	HCP	18.75	1.35	720	1.94	10.5	26.0	L
68	Er	HCP	18.46	1.34	1230	2.18	16.8	57.0	L
71	Lu	HCP	17.77	1.31	750	1.85	12.8	34.5	L

The notation for the lattice types and probable phase states is the same as in Table I (R—rhombohedral).

cated in the right-hand part of Table II. In the case of La it takes place at $\sigma_c = 1.51$, and in the case of all other rare earth metals at σ_c close to 1.9.

In Ce, all the dynamic experimental data pertain to the low-compressibility high-pressure α phase. As is well-known[22,39], the γ-α electronic transition in cerium occurs at relatively low pressure, 7 kbar. The two isomorphic phases differ from each other in specific volume. The phase-equilibrium line separating them on the P-T diagram at 18 kbar and 280°C is terminated by a critical point, above which strong discontinuities on the dilatometric curves and on the electric resistance curves are not recorded. As established by neutron diffraction[40] and also by measurements of the Hall effect[39], the formation of a dense α phase is due to the transition of its only f electron to the d-band and to the consequent increase of the valence of Ce from 3 to 3.67.

In order to understand the causes of the electronic changes in Ce, we recall[24,41] that the electronic structure of the atoms of rare-earth elements has the following form: closed Xe shell, incomplete 4f layer, and finally, the $6s^2$ and $5d^1$ valence electrons. The 4f electrons are reliably screened by an outer closed layer of the $5s^25p^6$ shell of Xe, inasmuch as the 4f layer has a much smaller average radius. In view of all this, we expect that the 4f electrons in the crystal in the unexcited state are practically not collectivized, do not influence the binding forces, the valence, and the limiting electron density.

A comparison of the interatomic distances in divalent rare earth metals (Eu, Yb), and in trivalent and tetravalent (γ-Ce) shows that under normal conditions the atomic volumes decrease with increasing number of valence electrons[41]. Therefore application of external pressures can stimulate the transition of the 4f electrons to the conduction band, formed by the s-d electrons.

The reasons why such—d transitions at low pressures occur only in the case in Ce are not clear at the present time. In the case of Lu, which has a stable configuration of the filled s-layer, the discontinuous decrease of the compressibility is uniquely explained by the displacement of the outer 6s electrons to the d levels of the fifth layer. Apparently, in other rare-earth metals the formation of low-compressibility

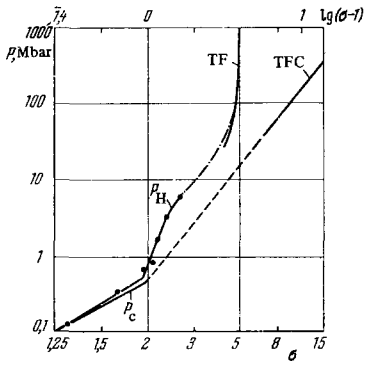

FIG. 20. Extrapolation of shock adiabat and zero isotherm of Sm. —·— —interpolation section of dynamic adiabats; — — —interpolated section of zero isotherm; TF—shock adiabat calculated from the Thomas-Fermi theory [42]; TFC—zero isotherm calculated from the TFC theory.

electron configurations is connected primarily with the displacement of the s electrons to the 4f and 5d levels, which lie close in energy.

VII. CONCLUSION

Extensive investigations with the aid of shock waves revealed the main laws governing the compressibility of metals having different electronic structures at high pressures. It turned out that the resistance of metals to compression depends principally on the magnitude of their atomic volumes, or, in other words, on the average electron density on the boundaries of the compressed atoms. There is no direct correlation between the binding energy and the compressibility, and the elasticity of metals is connected with the coupling forces only to the extent that these forces determine the interatomic distances and the atomic volumes.

In many metals, in experiments with shock waves, the shock-compression curves revealed sharp kinks when the density was increased by 1.5—2.5 times, evidencing a discontinuous increase of the elasticity of the metal. The data presented in the present review show that these singularities are observed in practically all metals of the large periods, pertaining to the first five A-groups, i.e., to the alkali, alkali-earth, rare-earth, and transition metals, which occupy the uppermost positions and the decreasing branches of the atomic-volume curve. The atoms of these elements, under normal conditions, have unoccupied or little-filled internal d-shells. The repopulation of the outer s-electrons to the d-levels causes formation of denser and low-compressibility electron configurations with an increased number of the binding d-electrons. The completion of the electron-transition process is naturally associated with the kinks, at which two smooth sections of the dynamic adiabats intersect. The large compressibility in the first compression phase is due not only to the low density of the external s-electrons, but also to their gradual displacement within the atom upon compression, thus decreasing additionally the limiting density of the electron cloud.

There exist causes, indicated in Chapter II, which violate the correspondence between the configurations of the shock adiabats and the equilibrium zero isotherms in the region of electronic transitions. One of these causes is the high temperature of dynamic compression, causing excitation of the electrons and additional smearing of their energy bands. Another cause is connected with possible inertia of the electronic transitions, which apparently have a certain activation energy[33].

Hysteresis phenomena, which characterize the kinetics of electronic transformations and are of independent interest, were observed by x-ray diffraction in the study of Ce[42], and also of Rb[43] (using its electric-resistance curves). The strong disparity between the critical pressures of the transition in the compression and decompression waves was registered in[19] for Ca. These factors lead to a smoothing, on the adiabats, of the singularities characteristic of equilibrium zero isotherms. In particular, under their influence, the steplike form of the compression curve, shown in Fig. 2b and characteristic of first-order

phase transitions, may become less noticeable in dynamic experiments.

A significant result of the dynamic experiments is the determination, in a wide range of pressures, of the upper branches of the adiabats, which characterize the modified electronic structure of the metal. Knowledge of the Hugoniot adiabats in this region makes it possible to extrapolate them with sufficient accuracy to "quantum-statistical" pressures of several hundred Mbar, at which the statistical theory of the atom becomes valid. The result of such extrapolations is shown in Fig. 20 for the dynamic adiabat and the zero isotherm of Sm.

The theoretical branches of the cold curve were calculated in accordance with the TFC theory (Thomas-Fermi model with corrections)[20], and the adiabats were calculated in accordance with the "hot Thomas-Fermi" theory[44] with allowance for the thermal contribution of the ions, treated as an ideal gas, and of the "cold" components from[20].

In spite of the large gaps between theory and experiment, the uncertainty of the constructed interpolated sections of the curves is small. This statement holds true to an even larger degree for metals with smooth compression curves[1,9,11,32,45].

[1] L. V. Al'tshuler, Usp. Fiz. Nauk 85, 197 (1965) [Sov. Phys.-Usp. 8, 52 (1965)].

[2] Ya. B. Zel'dovich and Yu. P. Raĭzer, Fizika udarnykh voln i vysokotemperaturnykh gidrodinamicheskikh yavlenii (Physics of Shock Waves and High-temperature Hydrodynamic Phenomena), Fizmatgiz, 1963.

[4] L. V. Al'tshuler, K. K. Krupnikov, B. N. Ledenev, V. I. Chuchikhin, and M. I. Brazhnik, Zh. Eksp. Teor. Fiz. 34, 874 (1958) [Sov. Phys.-JETP 7, 606 (1958)].

[5] L. V. Al'tshuler, K. K. Krupnikov, and M. I. Brazhnik, ibid. 34, 886 (1958) [7, 614 (1958)].

[6] L. V. Al'tshuler, S. B. Kormer, M. I. Brazhnik, L. A. Vladimirov, M. P. Speranskaya, and A. I. Funtikov, ibid. 38, 1061 (1960) [11, 766 (1960)].

[7] L. V. Al'tshuler, S. B. Kormer, A. A. Bakanova, and R. F. Trunin, ibid. 38, 790 (1960) [11, 573 (1960)].

[8] R. G. McQueen and S. P. Marsh, J. Appl. Phys. 31, 1253 (1960).

[9] L. V. Al'tshuler, A. A. Bakanova, and R. F. Trunin, Zh. Eksp. Teor. Fiz. 42, 91 (1962) [Sov. Phys.-JETP 15, 65 (1962)].

[10] K. K. Krupnikov, M. I. Brazhnik, and K. K. Krupnikova, ibid. 42, 675 (1962) [15, 470 (1962)].

[11] S. B. Kormer, A. I. Funtikov, V. D. Urlin, and A. N. Kolesnikova, ibid. 42, 686 (1962) [15, 477 (1962)].

[12] C. Skidmore and E. Morris, Proceedings of Symposium, Vienna, May 1962.

[13] K. K. Krupnikov, A. A. Bakanova, M. I. Brazhnik, and R. F. Trunin, Dokl. Akad. Nauk SSSR 148, 1302 (1963) [Sov. Phys.-Dokl. 8, 203 (1963)].

[14] M. H. Rice, J. Phys. and Chem. Solids 26, 483 (1965).

[15] A. A. Bakanova, I. P. Dudaladov, and R. F. Trunin, Fiz. Tverd. Tela 7, 1615 (1965) [Sov. Phys.-Solid State 7, 1307 (1965)].

[16] L. V. Al'tshuler, A. A. Bakanova, and I. P. Dudoladov, ZhETF Pis. Red. 3, 483 (1966) [JETP Lett. 3, 315 (1966)].

[17] A. A. Bakanov and I. P. Dudoladov, ibid. 5, 322 (1967) [5, 265 (1967)].

[18] R. E. Duff, W. H. Gust, E. B. Royce, A. C. Mitchell, R. N. Keeler, and W. G. Hoover, Symposium High Dynamic Pressure, Paris, September 1967.

[19] L. V. Al'tshuler, A. A. Bakanova, and I. P. Dudoladov, Zh. Eksp. Teor. Fiz. 53, 1967 (1967) [Sov. Phys.-JETP 26, 1115 (1968)].

[20] N. M. Kalitkin, Zh. Eksp. Teor. Fiz. 38, 1534 (1960) [11, 1106 (1960)].

[21] L. F. Vereshchagin and A. I. Likhter, Dokl. Akad. Nauk SSSR 86, 745 (1952).

[22] V. V. Evdokimova, Usp. Fiz. Nauk 88, 93 (1966) [Sov. Phys.-Usp. 9, 54 (1966).

[23] A. S. Kompaneets, Teoreticheskaya fizika (Theoretical Physics), 2d Ed., Gostekhizdat, 1957.

[24] S. V. Vonsovskiĭ, and Yu. A. Izyumov, Usp. Fiz. Nauk 77, 377 (1962) [Sov. Phys.-Usp. 5, 547 (1963)].

[25] E. S. Alekseev, and R. G. Arkhipov, Fiz. Tverd. Tela 4, 1077 (1962) [Sov. Phys.-Solid State 7, 795 (1962)].

[26] G. M. Gandel'man, Zh. Eksp. Teor. Fiz. 51, 147 (1966) [Sov. Phys.-JETP 24, 99 (1967)].

[27] R. D. Arkhipov, Zh. Eksp. Teor. Fiz. 49, 1601 (1965) [Sov. Phys.-JETP 22, 1095 (1966)].

[28] U. Dehlinger, Theoretical Metallurgy (Russ. Transl.), State Publishing House for Ferrous and Nonferrous Metallurgy, 1960.

[29] F. Seitz, The Modern Theory of Solids, McGraw-Hill, 1940.

[30] I. M. Lifshitz, Zh. Eksp. Teor. Fiz. 38, 1569 (1960) [Sov. Phys.-JETP 11, 1130 (1960)].

[31] G. M. Gandel'man, ibid. 43, 131 (1962) [16, 94 (1963)].

[32] R. L. Rosenberg and B. J. Alder, Metallurgy at High Pressures and High Temperatures, New York-London, 1964.

[33] Solids under Pressure, Ed. William Paul, Douglas M. Warschauer, New York, 1963.

[34] A. H. Jones, W. M. Isbell, and C. J. Maiden, J. Appl. Phys. 37, 3493 (1966).

[35] T. R. Butkowich, Geophys. Rev. 70, (1965).

[36] L. V. Al'tshuler, B. N. Moĭseev, L. V. Popov, G. V. Simakov, and R. F. Trunin, Zh. Eksp. Teor. Fiz. 54, 785 (1968) [Sov. Phys.-JETP 27, 420 (1968)].

[37] R. A. Stager and H. G. Drickamer, Phys. Rev. 131, 2524 (1963).

[38] P. W. Bridgman, Proc. Amer. Acad. Arts. Sci. 81, 165 (1952).

[39] A. Blandin, B. Cogblin, and Y. Fredel, I. Intern. Conf. on Physics of Solids at High Pressures, Tiscon, Arisona, p. 233, 1965.

[40] M. K. Wilkinson, H. R. Child, C. J. McHargue, W. C. Koehler, and E. O. Wollan, Phys. Rev. 122, 1409 (1961).

[41] V. G. Grigorovich, Mendeleev's Periodic Law and the Electronic Structure of Metals (Russ. Transl.), Mir, 1965.

[42] V. V. Evdomikova, X-ray Investigations of Certain Substances at Pressures up to 20 kbar, Dissertation, High-pressure Physics Institute, USSR Academy of Sciences, 1966.

[43] F. P. Bundy, Phys. Rev. 115, 274 (1959).
[44] R. Latter, Phys. Rev. 99, 1854 (1955).
[45] N. M. Kalitkin and I. A. Govorukhina, Fiz. Tverd. Tela 7, 355 (1965) [Sov. Phys.-Solid State 7, 287 (1965)].

Translated by J. G. Adashko